Tuijin Jishu/Journal of Propulsion Technology
ISSN: 1001-4055
Vol. 44 No. 5 (2023)

Synthesis and Characterization of Zno Nanostructure by Hydrothermal Method

V. S. Kalyamwar[1*], S. D. Charpe[2], P.D. Shirbhate[3], R. B. Pedhekar[4]

*[*1] Department of Physics, Bharatiya Mahavidyalaya, Amravati, India.*

[2] Department of Physics, J. D. Patil Sangludkar Mahavidyalaya, Daryapur Dist. Amravati, India.

[3] Department of Physics, Gopikabai Sitaram Gawande Mahavidyalaya, Umarkhed Dist. Yavatmal, India.

[4]Mahatma Jyotiba Fule Commerce, Science & Vitthalrao Raut Arts College, Bhatkuli, Dist. Amravati, India.

Abstract:

Zinc oxide nanostructures were synthesized by hydrothermal method. The XRD spectrum indicates that the sample is wurtezite (hexagonal) structured ZnO with lattice constants of a = 3.249A^0, c = 5.206 A^0. The crystallinity and structure of these ZnO nanostructures were studied by X-ray diffraction. The morphologies of these synthesized nanostructures were analyzed by transmission electron microscope. Effect of sonication time on the morphology and particle size of resultant product were investigated.

Keywords: *Hydrothermal synthesis, Zinc oxide nanostructure.*

1. Introduction

Zinc Oxide has a relatively large direct band gap at room temperature. Advantages associated with a large band gap include higher breakdown voltages, ability to sustain large electric fields, lower electronic noise, and high-temperature and high-power operation. The band gap of ZnO can be varying by its alloying with magnesium oxide or cadmium oxide. Zinc oxide is promising materials for electronics or optoelectronics applications such as gas sensor, liquid crystal displays, solar cell, heat mirrors, surface acoustics wave devices etc [1-10].

To synthesize ZnO nanostructures, variety of techniques like spray pyrolysis, molecular beam epitaxy, chemical vapor deposition, hydrothermal method, pulsed laser deposition, sol-gel method, laser ablation [11-17] etc. have been widely used.

In the present study, ZnO nanostructures were synthesized by using hydrothermal method. The crystallinity and structure of these ZnO nanostructures were analyzed with the help of X-ray diffraction. The morphologies of these synthesized nanostructures were explored by transmission electron microscope.

2. Experimental

Hydrothermal Method

All chemicals were of analytical grade and were used as purchased without further purification.

In present work, 5.2 g of Zinc acetate dehydrate was dissolved in 480 ml of distilled water. Subsequently, 20ml of 2M NaOH aqueous solution was introduced into the above aqueous solution drop by drop with constant stirring. The obtained mixture was kept at room temperature for 05 min, and then transferred in to 700ml Teflon-lined stainless steel reactor (autoclave), maintained at temperature 120 ^{0}C for 6 hrs and then cooled to room temperature naturally. After this process, the resultant white solution was collected in a beaker. The obtained white solution were sonicated (Ultrasonic wave treatment) with plus rate 4s and power 0.7A for

different time periods ranging from 30 min to 120 min. The resultant products were collected by centrifugation, washed several times with distilled water and ethanol and dried at temperature 70 ^{0}C for 3hrs. Synthesized ZnO nanostructure which was sonicated for 30 min, 60 min, 90 min and 120 min time period treated as 30 min ZnO, 60 min ZnO, 90 min ZnO and 120 min ZnO respectively.

3. Results and discussion

X-ray diffraction

X-ray diffraction data for structural characterization of various products synthesized by hydrothermal method were collected on the Philips PW 1710 X-ray diffractometer using Cu-Kα source. X-ray diffraction patterns of synthesized samples are helpful in studying the crystalline structure and determination of crystallite size.

The room temperature XRD patterns of synthesized 30 min ZnO, 60 min ZnO, 90 min ZnO and 120 min ZnO were shown in figure 1(a)-(d).

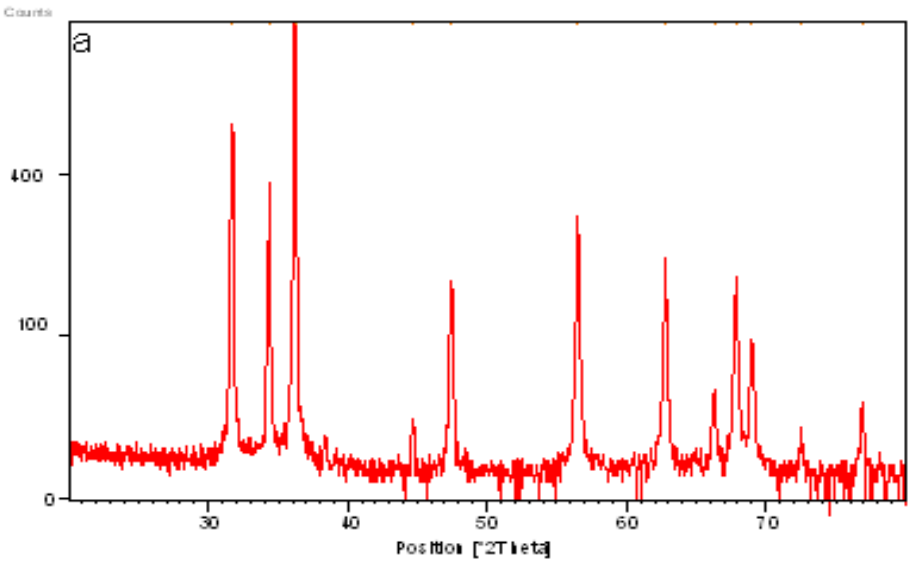

Figure 1(a) powder XRD pattern of 30 min ZnO synthesized by hydrothermal route

Figure 1(a) shows the powder XRD pattern of the ZnO nanostructure synthesized by hydrothermal route followed by 30min sonication. This XRD pattern shows that, all the diffraction peaks in the pattern can be assigned to hexagonal 'wurtzite' ZnO with lattice constants a= 0.3249 nm and c = 0.5206 nm, which are in good agreement with the literature values (JCPDS card No. 36-1451). In above XRD pattern, extra pick appear at 2θ = 44^0. This peak was identified as surface hydroxyl groups, which can be related to the formation of water on the ZnO nanostructure surface [18]. The XRD patterns of the ZnO nanostructures [figure 1(b)-(d)] with different sonication time show parallel results.

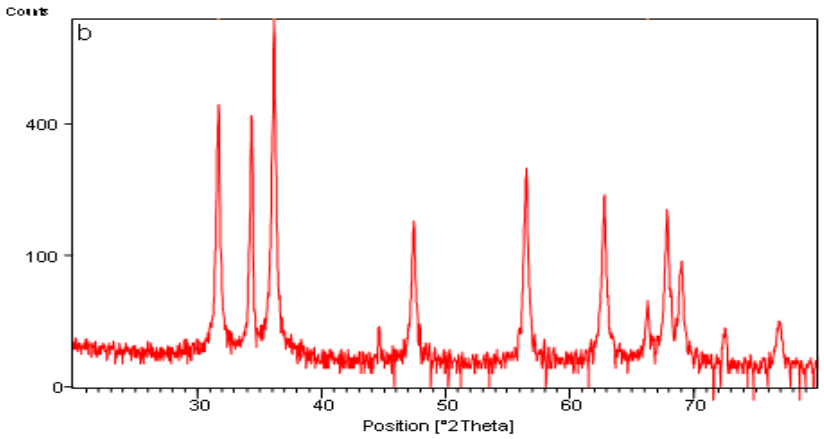

Figure 1(b) powder XRD pattern of 60 min ZnO synthesized by hydrothermal route

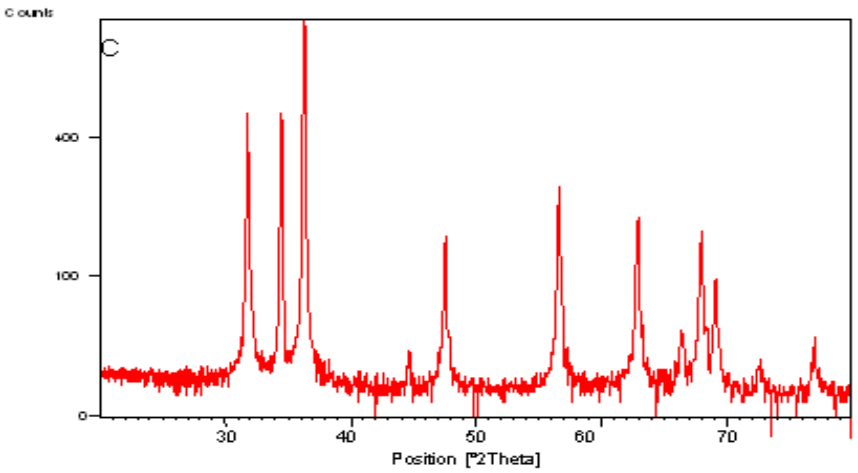

Figure 1(c) powder XRD pattern of 90 min ZnO synthesized by hydrothermal route

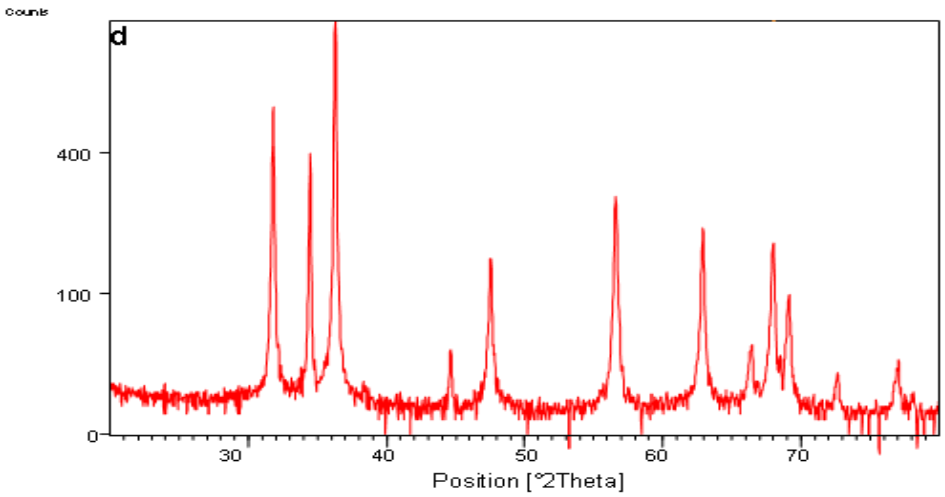

Figure 1(d) powder XRD pattern of 120 min ZnO synthesized by hydrothermal route

The following table shows the comparison of obtained XRD data with standard data (JCPDS card No. 36-1451).

Table 1 comparison of standard and observed 2θ &'d' of synthesized samples

Sample	Observed		Standard (JCPDS card No. 36-1451)		(h k l) Plane
	2θ	'd' Values (A^0)	2θ	'd' Values (A^0)	
30 min ZnO	31.7107	2.81944	31.770	2.8143	(1 0 0)
	34.3639	2.60759	34.422	2.6033	(0 0 2)
	36.2098	2.47878	36.253	2.4759	(1 0 1)
60 min ZnO	31.7226	2.81841	31.770	2.8143	(1 0 0)
	34.3645	2.60754	34.422	2.6033	(0 0 2)
	36.1692	2.48147	36.253	2.4759	(1 0 1)
90 min ZnO	31.7956	2.81211	31.770	2.8143	(1 0 0)
	34.4920	2.59819	34.422	2.6033	(0 0 2)
	36.3101	2.47216	36.253	2.4759	(1 0 1)
120min ZnO	31.8304	2.80998	31.770	2.8143	(1 0 0)
	34.4795	2.59910	34.422	2.6033	(0 0 2)
	36.3036	2.47258	36.253	2.4759	(1 0 1)

The influence of the sonication time on the particle size product was the main subject of interest here. To extract more information on the crystallinity, the XRD data is exercised to determine the crystallite size. The full width at half maxima (FEHM) of the intense (101) peak was evaluated for all the ZnO nanostructures, by using Scherrer's formula [19].

$D = k\lambda/\beta\sin\theta$

Where λ is the wavelength of incident beam (1.5406 A^0), β is the FWHM of the peak in radians, θ is the diffraction angle and k is Scherrer constant.

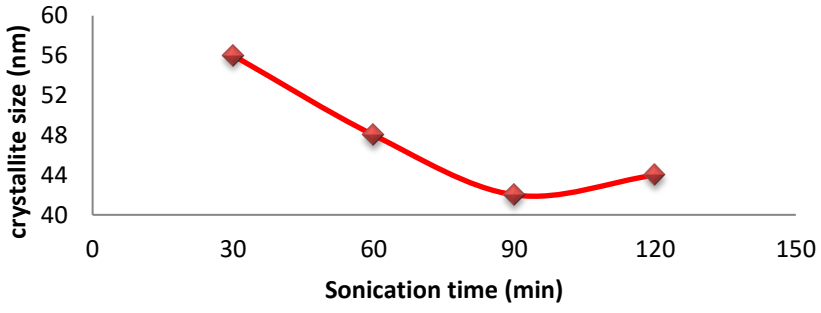

Figure 2 variation of crystallite size with sonication time.

Figure 2 shows the variation of crystallite size of synthesized ZnO with its sonication time. It is seen that crystallite size decreases with sonication time, conquer minimum value (42 nm) at 90 min sonication time and for further higher sonication time it increases. The increase in crystallite size with increasing sonication time beyond 90 min may be due to accumulation of ZnO nanoparticles to form crystallite of higher size.

Transmission electron microscope

The morphology and particle size of ZnO samples synthesized by hydrothermal method were examined by using Techai G2 20 Ultra-Twin transmission electron microscope (Pune University, Pune). For the TEM observation, the as-prepared samples were added into an alcohol solution and subjected to violent ultrasonic stirring for hours; subsequently, a drop of this solution was dipped on a copper grid used for the TEM observation.

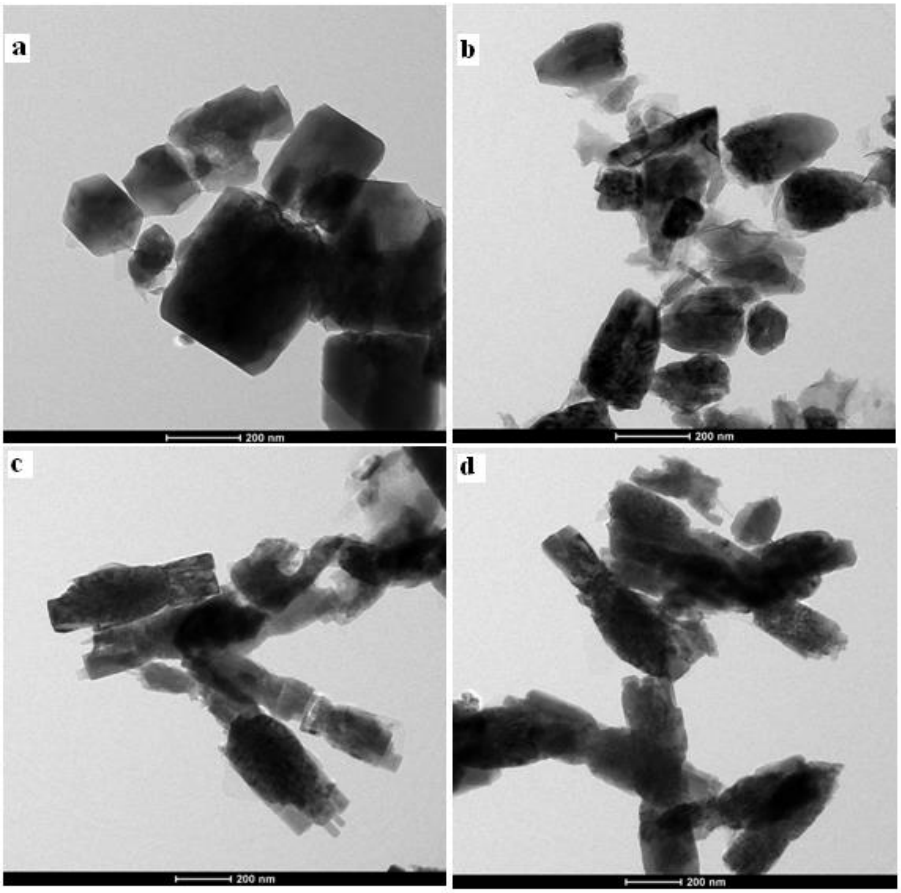

Figure 3 TEM images of a) 30 min ZnO, b) 60 min ZnO, c) 90 min ZnO, d) 120 min ZnO

Figure 3 illustrates the representative morphologies of the samples obtained by the hydrothermal synthesis followed by different sonication time from the same kind of precursor solution as mentioned in the experimental section. Figure 3(a) shows the formation of highly crystalline nanoparticles by hydrothermal method followed by 30min sonication. Figure 5(a)-(d) shows that as the sonication time increases, nanoparticles get converted into small dumbbell like nanorods. Figure 5(c) shows dumbbell like nanorods with average diameter of 40-45nm and length of 200-400nm.

Zinc oxide nanostructure growth mechanism

In hydrothermal process, at the beginning $Zn(OH)_2$ get precipitate, when zinc acetate react with sodium hydroxide. Precipitated $Zn(OH)_2$ will be dissolved to considerable extent to form ions of Zn^{2+} and OH^-, once the product of Zn^{2+} and OH^- exceeds a critical value which is necessary for the formation of ZnO crystals, the ZnO crystals will precipitate from the solution via the following chemical reaction.

$Zn(OH)_2 \rightarrow Zn^{2+} + 2OH^-$

$Zn^{2+} + 2OH^- \rightarrow ZnO + H_2O$

At the initial stage of hydrothermal process, the concentration of Zn^{2+} and OH^- were relatively higher so that the crystal growth in different direction was considerable, thus resulting in formation of ZnO particles.

Form the results of XRD it is clear that ZnO synthesized by hydrothermal method followed by 90 min sonication yield the product with Small crystalline size. These products with small crystallite size and innovative morphology can be used as sensor elements.

5. Conclusion

From the results obtained, following statements can be made for the synthesized ZnO nanostructures by hydrothermal and chemical route method.

1. Zinc oxide nanostructures synthesized by hydrothermal method shows highly crystalline in nature with hexagonal wurtzite structure with lattice constants a= 0.3249 nm and c = 0.5206 nm.
2. Zinc oxide nanostructures synthesized by hydrothermal followed by 90 min sonication has the lowest crystallite size 48nm among other synthesized nanomaterials.

References :

[1] Chopra L., Major S., Panday D. K., Thin Solid Films 1021 (1983) 1-4.
[2] Bose S., Barua A. K., Journal of Physics D: Applied Physics 32 (1999) 213-218.
[3] Kim H., Gilmore C. M., Applied Physics Letters 76 (2000) 259-261.
[4] Xia Y., Hu C. G., Han X. Y., Xiong Y. F., Gao P. X., Liu G. B., Solid State Communications 141 (2007) 506–509.
[5] Ki Won Kim, Pyeong Seok Cho, Sun Jung Kim, Jong Heun Lee, Chong Yun Kang, Jin Sang Kim, Seok Jin Yoon, Sensors and Actuators B 123 (2007) 318–324
[6] Forleo A., Francioso L., Capone S., Siciliano P., Lommens P., Hens Z., Sensors and Actuators B 146 (2010) 111–115.
[7] Badadhe Satish S., Mulla I.S., Sensors and Actuators B 143 (2009) 164–170.
[8] Lupan O.I., Shishiyanu S.T., Shishiyanu T.S., Superlattices and Microstructures 42 (2007) 375–378.
[9] Sarala Devi G., Bala Subrahmanyam V., Gadkari S.C., Gupta S.K., Analytica Chimica Acta 568 (2006) 41–46.
[10] Ravi Chand Singh, Onkar Singh, Manmeet Pal Singh, Paramdeep Singh Chandi, Sensors and Actuators B 135 (2008) 352–357.
[11] Shinde V. R., Lokhande C. D., Mane R. S., Han S. H., Applied Surface Science 245 (2005) 407-413.
[12] Morgan J. H., Broide D. E., Canadian Journal of Physics 60 (1982) 1387-1390.
[13] Craciun V., Elders J., Gardeniers J. G. E., Geretovsky J., Boyd I. W., Thin Solid Films 259 (1995) 1-4.
[14] Ohyama M., Kozuka H., Yoko T., Thin Solid Films 306 (1997) 78-85.
[15] Ayouchi R., Leinen D., Martin F., Gabas M., Dalchiele E., Ramos Barrado J. R., Thin Solid Films 426 (2003) 68-77.
[16] Paraguay F., Morales J., Estrada W., Andrade E., Yoshida M. M., Thin Solid Films 366 (2000) 16-27.
[17] Moustaghfir A., Tomasella E., Amor S. B., Jacquet M., Cellier J., Sauvage T., Surface and Coating Technology 193 (2003) 174-175.
[18] Kester W J Wong, Matthew R Field, Jian Zhen Ou, Kay Latham, Michelle J S Spencer, Irene Yarovsky, Kourosh Kalantar-zadeh, Nanotechnology 23 (2012) 015705-015713
[19] Hilber T., Letonja P., Marr R., Poit P., Siebenhofer M. Part. Part. Syst. Charact. 19 (2002) 342-347.